

Continuous wave laser-induced forward transfer of conductive Ag nanoparticle inks

Author: Sergio González-Torres*

Advisor: Pere Serra Coromina

Departament de Física Aplicada, Facultat de Física, Universitat de Barcelona, Martí i Franquès 1, 08028 Barcelona, Spain.

Abstract: The laser induced forward transfer of silver nanoparticle ink using continuous wave laser is studied in this work. The feasibility of this method for printing well-defined lines is proven. Line formation is studied in the laser intensity - scan speed parameter space, showing satisfactory results for a range of energies and speeds. The conductivity of the lines was measured to be comparable to those obtained with inkjet printing, proving the effectiveness of this technique to produce functional electrical interconnects. High speed photography of the transfer process is performed, revealing the markedly different transfer dynamics compared to the traditional, pulsed laser LIFT process.

I. INTRODUCTION

Several approaches to material deposition are available. Owing to its already extended use in the printing of documents and graphics, inkjet printing emerged as a technique for the transfer of materials. Current inkjet technology is based on the ejection of ink through a 20-30 μm nozzle, propelled by means of heating or by piezoelectric actuators [1]. Despite the advantages it offers as a mature method, the constraints that a nozzle-based system like inkjet printing present serious drawbacks for the printing of certain types of ink. The nozzle is not only subject to issues like obstruction due to ink drying [1], but it also limits the range of materials that can be transferred successfully. These include inks whose particle size is bigger than about 100 nm [1]. Also, restrictions on ink viscosity and surface tension further limit the range of printable inks [1]. Thus, should the nozzle and its limitations be removed from the picture, a wider range of materials could be printed with fewer restrictions.

Laser induced forward transfer (LIFT) does not involve the use of a nozzle, thus liberating constraints and allowing printing novel inks. FIG. 1 illustrates the standard LIFT setup, consisting of a transparent substrate coated with the target material. Upon irradiation by a laser pulse, a jet of ink is formed, which advances towards the acceptor substrate, placed close to the donor [2]. As the jet contacts the receiving substrate, a small drop of ink is deposited. One of the main concerns in LIFT printing is the preservation of the target material's properties after irradiation. For the deposition of simple materials that can undergo phase changes in the transfer process without modification in their properties after deposition, no additional considerations beyond the material deposition mechanism are required. However, further attention is needed for materials that might undergo undesired changes upon irradiation, such as oxidation [2]. These problems can be avoided using different variations of the technique, including [2]: the use of a Dynamic Release Layer (DRL) and the use of inks. These modifications to LIFT allow printing materials without direct alterations, preserving the properties of delicate materials.

Traditionally, LIFT involves the use of a pulsed laser to irradiate a donor substrate, placed close to an acceptor substrate. The dynamics of classic LIFT ink printing have been thoroughly investigated and are well understood [3-6]. This process consists on the formation of a cavitation bubble by

means of a short laser pulse, which propels a stable jet of ink that eventually contacts the acceptor substrate and deposits a drop of ink. In pulsed LIFT printing an energy threshold is observed, where lower pulse energies yield no ink deposition. This energy threshold can be originated from two different phenomena: the energy threshold to produce a jet, and the energy threshold for the produced jet to reach the acceptor substrate [4,7]. Depending on experimental conditions, the observed threshold corresponds to one of the two.

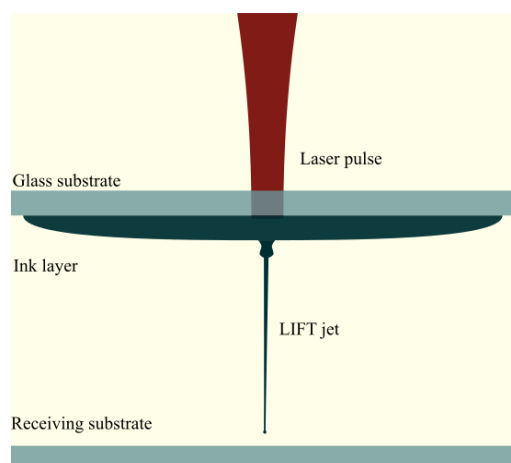


FIG. 1: Classic pulsed LIFT printing, wherein a single laser pulse originates a single stable ink jet at a time.

Until the present, LIFT printing has been studied with pulsed lasers with pulse durations in the range of ns or lower [1,3,4,7]. Pulsed lasers, however, are much more expensive than their continuous wave (CW) counterparts. Thus, if CW lasers are proven to be effective at transferring inks, the cost associated with a LIFT printing setup could diminish considerably.

In this work, an alternative mode of LIFT employing a continuous wave laser is studied. The transfer dynamics of such a process are expected to differ widely from the known fluid mechanics of pulsed laser LIFT printing, since the idea of the formation of a bubble that projects a stable jet is based on the premise of a single short pulse interacting with the donor material at any given time. The feasibility of this technique is demonstrated through the printing of long, well defined continuous lines, and the posterior characterization of printed lines in terms of electrical resistance and thickness. Finally, the dynamics of CW-LIFT printing will be studied using a fast photography setup.

* Electronic address: sgonzat011.alumnes@ub.edu

II. EXPERIMENTAL SETUP

The laser used in this work is an Nd:YAG unit (Baasel Lasertech, LBI-6000) working at wavelength of 1064 nm, with a beam waist diameter of 100 μm and operating in CW mode. The laser beam can be deflected with micrometric resolution in the x-y plane using a system of galvanometric mirrors and tuned to a scan speed between 0-600 mm/s. After the galvanometric head, a 100 mm lens is used to focus the beam onto the sample, as illustrated in FIG 2

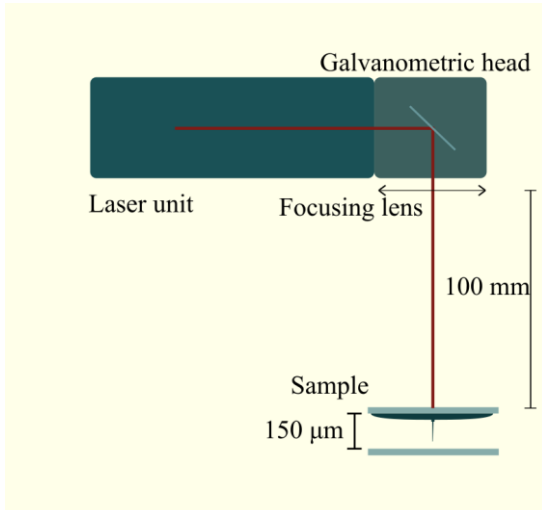


FIG. 2: Setup for LIFT used in this work. The sample is placed at the waist of the laser beam, and the acceptor and receiver substrates are separated using two 150 μm thick spacers.

The ink used in this work is a commercial Ag nanoparticle ink (Sigma Aldrich, ref. 36481) with a particle size <50nm, solid content 30-35 %wt, density 1.45 g/cm³ and viscosity 8-10 mPa·s. The morphology of the samples is analyzed with optical microscopy using a Carl Zeiss microscope, model AX10 Imager.A1. Sample profiles are measured with a Sensofar PL μ 2300 confocal microscope. High speed images are captured with an AOS Technologies AG, model S-PRI F1 1000 fps camera, furnished with a 10x, NA = 0.28 microscope objective lens placed close to the donor substrate. The high-speed imaging setup was illuminated with a Thorlabs Inc, model OSL1-EC 150 W halogen lamp in a shadowgraphy configuration.

To produce a donor sample, 30 μL of ink are placed on one end of a 25x75 mm² microscope slide. The ink is then spread using a blade coater, covering a surface of about 25x45 mm². This spreading method tends to leave a bump of excess ink at the end, which is removed with a paper wipe. After coating, the average ink layer was weighted to an average of 35 mg, resulting in a layer of about 20 μm in thickness. The receiving substrate is an identical clean slide, separated from the first one by two microscope cover slides totaling a spacing of 150 μm . The sample is then placed so that the laser beam waist lie within the ink layer, with the donor substrate on top.

After printing, lines are sintered in an oven at 200 $^{\circ}\text{C}$ for one hour to improve conductivity. The tips of each line are coated with a conductive paste prior to the resistance measurements with a multimeter. The square resistance is calculated from line resistance using the following formula:

$$R_s = \frac{R \cdot W}{L} \quad (1)$$

Where W, L, and R are the line width, length and resistance, respectively.

III. RESULTS AND DISCUSSION

A. Characterization of CW-LIFTed lines

Lines were printed for an array of scan speeds and laser powers (150 to 600 mm/s and 0.16-14.87 W) on a single laser pass per line. In contrast to pulsed LIFT, a clear-cut printing power threshold is not observed (FIG. 3). Rather, there appears to be a progression from no material printed at the lowest powers, to increasing spray densities tracing the laser path as laser power increases until a certain laser power, above which fully formed lines are printed. This power threshold for full line formation appears to increase with increasing scan speeds, which is a consequence of the decreasing irradiation time. As scan speed increases, the time of irradiation of any point in the donor layer decreases, thus requiring a higher power to achieve a fully printed line.

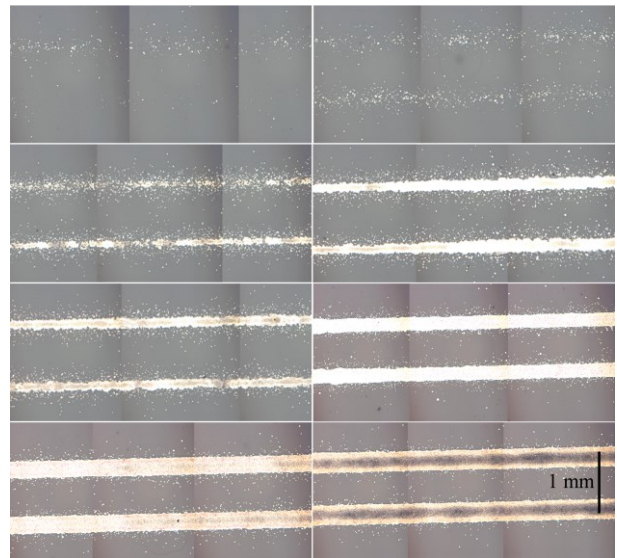


FIG. 3: Selection of reflection microscope images of pairs of lines for $v=300$ mm/s and laser powers 0.71, 0.86, 1.08, 1.30, 1.50, 2.31, 3.44, and 6.24 W. Notably, none of the lines present bulging. Spray is present around the lines, but it does not appear significant enough to cause short circuiting issues in a printed circuit. Well-formed lines of arbitrary length are obtained for laser powers as low as 1.3 W.

FIG 4 shows SEM images of the printed lines for different laser beam powers. Two distinct types of particles are observed: small particles, corresponding to unaltered Ag nanoparticles, and bigger ones, which are interpreted as aggregates of the original ink nanoparticles. For higher laser beam powers, fewer small particles cover the surface as the amount of particle aggregates increases. This decrease in the density of particles appears more pronounced for laser powers 5.8 W onwards.

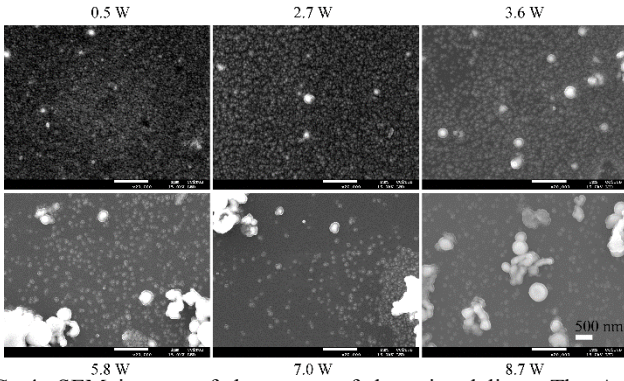


FIG. 4: SEM images of the center of the printed lines. The Ag nanoparticles covering the printed surface can be seen clearly. As laser power increases, the lines show a decrease in the area covered by the nanoparticles, as particle aggregates become more common. This decrease in particle number density is proposed as the reason behind the increase in resistance.

Sheet resistance and average thickness of the lines versus printing laser power for a scanning speed of $v=300$ mm/s are shown in FIG.5. Two complementary trends are observed: as the laser power increases, the deposited line thickness goes through a maximum to later decrease, while sheet resistance presents a minimum followed by a monotonous increase.

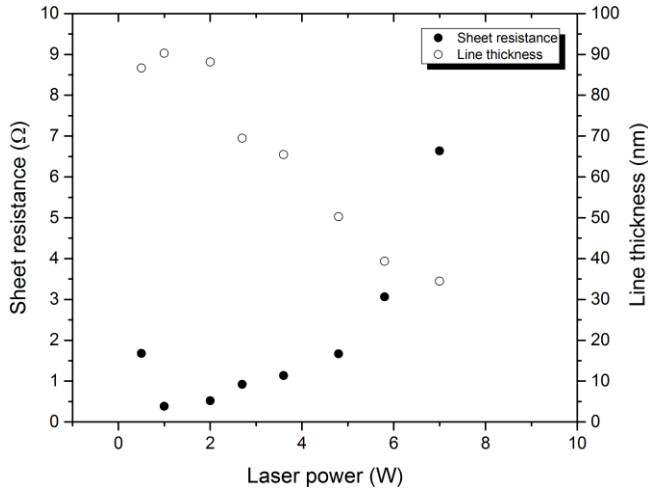


FIG. 5: Sheet resistance and average line thickness as a function of applied laser power for $v=300$ mm/s. Both plots show complementary trends: as thickness increases, sheet resistance decreases, presenting extrema for an applied power of 1 W. A sheet resistance of $80.9 \Omega_s$ and thickness of 26.6 nm are measured for a laser power of 8.7 W

The minimum sheet resistance ($0.38\Omega_s$) is obtained at a fairly low power of 1W. This result is significant, both because it is comparable to those obtained with inkjet printing [8], and because the use of lower power lasers could further diminish the costs associated with CW-LIFT printing. This, added to the fact that well defined lines are obtained for a range of laser powers and laser scanning speeds makes CW-LIFT suitable for printing interconnects for electric circuits.

A clear correlation between line resistance and nanoparticle concentration is observed. Coinciding with the notable decrease in nanoparticle concentration around a laser beam power of 5.8 W, a sharp increase in line sheet resistance can be seen. Thus, for higher laser powers, the ink is effectively overheated leading to the coalescence of particles

into clusters, decreasing the overall particle density and resulting in higher resistance values.

B. Fast photography of the CW-LIFT printing process

The image acquisition setup employed in this work does not require critical timing. The recording system was simply triggered by hand, after which the laser was activated with a slight delay. Afterwards, the recordings were cropped to remove the frames before and after the LIFT process. All recordings correspond with a donor substrate prepared in the same manner as for line printing but without an acceptor substrate underneath, with an aperture time of $5 \mu s$.

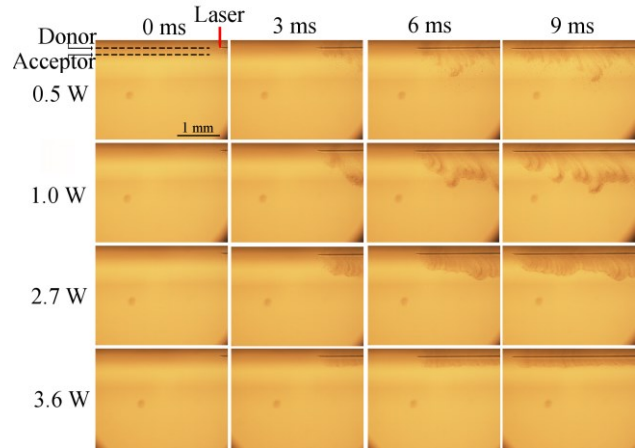


FIG. 6: Fast photography still shots of the CW-LIFT ejection process for four different laser powers. The donor substrate position and the eventual position of the acceptor substrate, $150 \mu m$ beneath the former, are shown. The laser beam scans in the left direction. Instead of the jetting mechanism typical of pulsed LIFT, a transfer dynamic closer to spraying is observed. Despite the apparent spray, well resolved lines like those of FIG 3 are obtained with repeatability, owing to the close spacing between donor and acceptor substrates.

The images show a transfer process akin to a spray, a mechanism that bears no resemblance with the dynamics of pulsed LIFT. This observation is significant: we have a type of ink transfer completely unlike what has been studied until now, yet it yields perfectly functional lines. This spraying dynamic can also explain the small droplets found around the printed lines.

To explain this new transfer mechanism, a pool-boiling description is proposed. As a result of the longer times of exposition resulting from the irradiation with a CW laser, compared to the pulsed LIFT case, a significant volume of the donor layer might be slowly heated by conduction resulting in a phenomenon similar to the boiling of water in a stove. In such a scheme, multiple bubbles would be produced, which upon bursting would produce the spray observed in the high-speed images.

To prove the plausibility of this hypothesis, several characteristic quantities will be estimated. Assuming a laser of uniform intensity with a laser beam waist diameter of $100 \mu m$ and at scanning speed of 300 mm/s, the time of irradiation of any region of the donor layer is about:

$$t_i \sim \frac{D_l}{v} \sim 330 \mu s \quad (2)$$

This time of irradiation is orders of magnitude superior to those of pulsed LIFT, which uses lasers with a pulse length of ns or lower. Now we will compare the penetration depth of the laser with the thermal penetration depth through conduction. The optical penetration depth can be approximated as:

$$l_{\text{opt}} = \sqrt{\frac{2\rho_e}{\omega\mu_0}} \sim 0.7 \mu\text{m} \quad (3)$$

The thermal penetration depth for an irradiation time t_i corresponds to:

$$l_{\text{th}} = \sqrt{\frac{2kt_i}{\rho_m c_p}} \sim 30 \mu\text{m} \quad (4)$$

The thermal penetration depth is clearly greater than the optical depth, thus the heating of the layer is dominated by thermal conduction, which diffuses the heat deep along its thickness. Now, the time required to give rise to boiling will be estimated. A nucleation size of $1 \mu\text{m}$ is assumed, chosen to lie halfway about the orders of magnitude of the particle size ($\sim 50 \text{ nm}$) and layer thickness ($\sim 15 \mu\text{m}$). In order to induce boiling in the ink layer, a temperature beyond the standard boiling point of water is needed. Combining the Clausius-Clapeyron and Young-Laplace equations [9], a formula for the required superheat is obtained:

$$\Delta T_{SH} = \frac{2\gamma T_s}{L\rho_v R} \sim 20 \text{ K} \quad (5)$$

This is the increase in temperature above the standard boiling point required for boiling to occur under these conditions. Thus, at standard temperature and pressure conditions, a temperature of $T_B = 393 \text{ K}$ is needed for pool boiling to occur. Lastly, knowing T_B , the time required to produce boiling can be approximated:

$$t_B = \frac{\pi\rho_m D_l^2 l_{th} c_p (T_B - T_0)}{4W} \sim 8 \mu\text{s} \quad (6)$$

Where the irradiated volume corresponds with:

$$V_{\text{irr}} = \frac{D_l^2 \pi l_{th}}{4} \quad (7)$$

The time of irradiation t_i obtained earlier is much greater than t_B , indicating that boiling is likely to happen for about the same length of time the region is irradiated. Thus, any area that is illuminated by the laser in this manner can undergo pool boiling. This proves the plausibility of pool boiling being the main mechanism involved in CW LIFT printing.

IV. CONCLUSIONS

The feasibility of a novel approach to ink laser induced forward transfer using a continuous wave laser instead of a

pulsed one for the printing of Ag nanoparticle ink lines is proven in this work.

Through the characterization of the lines in terms of average thickness and square resistance, CW-LIFT was proven to be effective at printing functional electrical interconnects, comparable to those obtained through inkjet printing but without the constraints of a nozzle-based system. A notably low optimal printing power of $\sim 1 \text{ W}$ was found, where sheet resistance was measured to be minimal. Higher powers yield worse results, and around 3 W the lines present diminishing concentrations of particles as a result of overheating-induced coalescence of the individual particles into aggregates, as assessed through SEM imaging of the center of the lines.

The transfer mechanism of CW LIFT was examined using a 1000 fps capturing setup, revealing a process completely dissimilar to traditional LIFT consisting of spraying dynamics. To explain this unusual mechanism, pool-boiling is proposed as the main cause. This pool-boiling hypothesis is proven plausible after calculating several relevant characteristic figures.

V. APPENDIX

A. Parameters used in the calculations of section III.B

Ink		
Electrical resistivity	ρ_e	$5 \cdot 10^4 \Omega \cdot \text{m}$
Mass density	ρ_m	$1.45 \cdot 10^3 \text{ kg/m}^3$
Specific heat	c_p	$245 \text{ J/(kg}\cdot\text{K)}$

Water		
Thermal conductivity	κ	$0.591 \text{ W/(m}\cdot\text{K)}$
Surface tension (373 K)	γ	0.059 N/m
Latent heat	L	$2.26 \cdot 10^6 \text{ J/kg}$
Density of vapor	ρ_v	1 kg/m^3
Density of water	ρ_L	10^3 kg/m^3
Thermal conductivity	κ	$0.591 \text{ W/(m}\cdot\text{K)}$
Boiling point at 1atm	T_s	373.15 K

Other		
Room temperature	T_0	300 K
Laser power	W	1 W
Laser beam waist diameter	D_l	$100 \mu\text{m}$
Laser scan speed	v	300 mm/s

Acknowledgments

I thank Dr. Pere Serra for his committed advisory work. I also would like to acknowledge the support my lab colleagues, especially Pol Sopeña for his valuable input and help in the laboratory, and my friends and family, especially Ferran Bonet.

-
- [1] P. Calvert, «Inkjet Printing for Materials and Devices,» *Chem. Mater.*, 10,13:3299-3305,2001.
- [2] C. B. Arnold, P. Serra i A. Piqué, «Laser Direct-Write Techniques for Printing of Complex Materials,» *MRS BULLETIN*, 32:23-31,2007.
- [3] A. Patrascioiu, J. M. Fernández-Pradas, A. Palla-Papavlu, J. L. Morenza i P. Serra, «Laser-generated liquid microjets: correlation between bubble,» *Microfluid Nanofluid*, 16:55–63,2014.
- [4] M. Colina, M. Duocastella, J. Fernández-Pradas, S. P. i J. Morenza, «Laser-induced forward transfer of liquids: Study of the droplet ejection,» *JOURNAL OF APPLIED PHYSICS*, 99,084909,2006.
- [5] M. Duocastella, J. M. Fernández-Pradas, J. L. Morenza i P. Serra, «Time-resolved imaging of the laser forward transfer of liquids,» *JOURNAL OF APPLIED PHYSICS*, 106,084907,2009.
- [6] R. Venkata Krishna Rao, K. Venkata Abhinav, P. S. Karthik i Surya Prakash Singh, «Conductive silver inks and their applications in,» *RSC Adv.*, 5,77760,2015.
- [7] M. Duocastella, A. Patrascioiu, J. Fernández-Pradas, J. Morenza i S. P., «On the correlation between droplet volume and irradiation,» *Appl Phys A*, 109:5–14,2012.
- [8] H.J. Gysling, Nanoinks in inkjet metallization - Evolution of simple additive-type metal patterning, *Curr. Opin. Colloid Interface Sci.* **2014**, 19, 155-162.
- [9] C. Brennen, Cavitation and bubble dynamics, New York: Oxford University Press, 1995.